



LUND UNIVERSITY

Transient Electromagnetic Wave Propagation in Anisotropic Dispersive Media

Fridén, Jonas; Kristensson, Gerhard; Stewart, Rodney D.

1992

[Link to publication](#)

Citation for published version (APA):

Fridén, J., Kristensson, G., & Stewart, R. D. (1992). *Transient Electromagnetic Wave Propagation in Anisotropic Dispersive Media*. (Technical Report LUTEDX/(TEAT-7023)/1-23/(1992); Vol. TEAT-7023). [Publisher information missing].

Total number of authors:

3

General rights

Unless other specific re-use rights are stated the following general rights apply:

Copyright and moral rights for the publications made accessible in the public portal are retained by the authors and/or other copyright owners and it is a condition of accessing publications that users recognise and abide by the legal requirements associated with these rights.

- Users may download and print one copy of any publication from the public portal for the purpose of private study or research.
- You may not further distribute the material or use it for any profit-making activity or commercial gain
- You may freely distribute the URL identifying the publication in the public portal

Read more about Creative commons licenses: <https://creativecommons.org/licenses/>

Take down policy

If you believe that this document breaches copyright please contact us providing details, and we will remove access to the work immediately and investigate your claim.

LUND UNIVERSITY

PO Box 117
221 00 Lund
+46 46-222 00 00

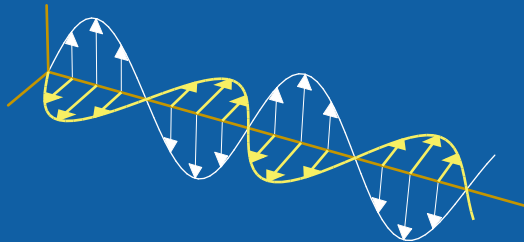
CODEN:LUTEDX/(TEAT-7023)/1-23/(1992)

Revision No. 2: June, 1993

Transient Electromagnetic Wave Propagation in Anisotropic Dispersive Media

Jonas Fridén, Gerhard Kristensson and Rodney D. Stewart

Department of Electrosience
Electromagnetic Theory
Lund Institute of Technology
Sweden



Jonas Fridén

Institute of Theoretical Physics
Chalmers University of Technology
University of Göteborg
S-412 96 Göteborg
Sweden

Gerhard Kristensson

Department of Electromagnetic Theory
Lund Institute of Technology
P.O. Box 118
SE-221 00 Lund
Sweden

Rodney D. Stewart

Department of Electromagnetic Theory
Royal Institute of Technology
SE-100 44 Stockholm
Sweden

Editor: Gerhard Kristensson

© Jonas Fridén, Gerhard Kristensson and Rodney D. Stewart, Lund, June, 1993

Abstract

In this paper transient electromagnetic wave propagation in a stratified, anisotropic, dispersive medium is considered. Specifically, the direct scattering problem is addressed. The dispersive, anisotropic medium is modeled by constitutive relations (a 3×3 matrix-valued susceptibility operator) containing time convolution integrals. In the general case, nine different susceptibility kernels characterize the medium. An incident plane wave impinges obliquely on a finite slab consisting of a stratified anisotropic medium. The scattered fields are obtained as time convolutions of the incident field with the scattering kernels. The scattering (reflection and transmission) kernels are uniquely determined by the slab and are independent of the incident field. The scattering problem is solved by a wave splitting technique. Two different methods to determine the scattering kernels are presented; an imbedding and a Green functions approach. Explicit analytic expressions of the wave front are given for a special class of media. Some numerical examples illustrate the analysis.

1 Introduction

There is a large variety of applications on electromagnetic wave propagation in anisotropic media. This has motivated studies since the beginning of this century. Some recent contributions on scattering by anisotropic media are found in Refs [6, 7, 18, 21] and on wave propagation in stratified anisotropic media in Refs [12, 19]. The analysis in these publications is made at fixed frequency. However, the development of, for example, pulse generators motivates a study of electromagnetic wave propagation problems in the time domain.

The objective of this paper is to develop a time domain formulation of scattering by an anisotropic, dispersive, stratified slab. It is a generalization of previous results obtained for transient electromagnetic wave propagation in isotropic dispersive media [1, 13] and the bi-isotropic case [14, 15]. The non-dispersive anisotropic case has been treated in Ref. [20].

The constitutive relations for a general linear, dispersive medium are analyzed in Ref. [9]. In this paper, the medium is modeled by a 3×3 matrix-valued susceptibility kernel χ , which is a function of time and depth in the medium.

In the direct scattering problem, which is of primary interest in this paper, a transient electromagnetic plane wave impinges obliquely on a slab of anisotropic medium, modeled by the known susceptibility kernel χ . The reflected and transmitted fields are the unknowns. These fields are readily calculated through time convolutions, once the reflection and transmission kernels are known. These kernels are the kernels of the integral operators that map the incident field to the reflected and the transmitted fields, respectively.

The basic tool for solving the scattering problem is the concept of wave splitting. This technique has been widely used during the last decade and a collection of the latest results is found in Ref. [5]. In free space, the wave splitting decomposes the field into its right and left moving parts. This concept has recently been generalized to higher dimensions, see Refs [22–24]. In the dispersive case for electromagnetic

fields in one spatial dimension, this decomposition becomes particularly simple, see [15].

Special attention is paid to the propagation of a finite jump discontinuity in the field, e.g., a wave front. It is proved that the propagation of the finite jump discontinuity is described by a 2×2 matrix. This matrix always exists for bounded susceptibility kernel $\boldsymbol{\chi}$, see Appendix A, and for some media there is an explicit analytic solution, see Appendix B.

2 Conversion of the Maxwell equations

The basic equations that model the macroscopic electromagnetic fields are the Maxwell equations. In a sourcefree region they are

$$\begin{cases} \nabla \times \mathbf{E}(\mathbf{r}, t) = -\frac{\partial \mathbf{B}(\mathbf{r}, t)}{\partial t} \\ \nabla \times \mathbf{H}(\mathbf{r}, t) = \frac{\partial \mathbf{D}(\mathbf{r}, t)}{\partial t} \end{cases} \quad (2.1)$$

The dynamics of the charges in the medium are modeled by the constitutive relations. In this paper constitutive relations with time convolutions are adopted. Moreover, for simplicity, the medium is assumed to have no optical response. More details on this model are given in Ref. [9]. Explicitly, the constitutive relations are

$$\begin{cases} \mathbf{D}(\mathbf{r}, t) = \epsilon_0 \left(\mathbf{E}(\mathbf{r}, t) + \int_{-\infty}^t \boldsymbol{\chi}(\mathbf{r}, t - t') \mathbf{E}(\mathbf{r}, t') dt' \right) \\ \mathbf{B}(\mathbf{r}, t) = \mu_0 \mathbf{H}(\mathbf{r}, t) \end{cases} \quad (2.2)$$

where the i th component¹ of the time convolution is defined as

$$\int_{-\infty}^t \boldsymbol{\chi}(\mathbf{r}, t - t') \mathbf{E}(\mathbf{r}, t') \big|_i dt' = \sum_{j=1}^3 \int_{-\infty}^t \chi_{ij}(\mathbf{r}, t - t') E_j(\mathbf{r}, t') dt'$$

The susceptibility kernel $\boldsymbol{\chi}$ is a matrix-valued function, which, due to causality, is identically zero for $t < 0$. For simplicity, $\boldsymbol{\chi}$ is assumed to be continuously differentiable for $t \geq 0$. No additional constraints on the matrix $\boldsymbol{\chi}$, at a given space-time coordinate, are imposed. A class of media of interest is the reciprocal media which correspond to a symmetric susceptibility matrix $\boldsymbol{\chi}$, see Ref. [9] and Section 7. The permittivity and the permeability of vacuum are denoted ϵ_0 and μ_0 , respectively, and the phase velocity c_0 and the wave impedance η_0 of vacuum are

$$c_0 = \frac{1}{\sqrt{\epsilon_0 \mu_0}}, \quad \eta_0 = \sqrt{\frac{\mu_0}{\epsilon_0}}$$

¹Both the notation (x, y, z) and $(1, 2, 3)$ are used, for a right handed cartesian coordinate system, throughout this paper.

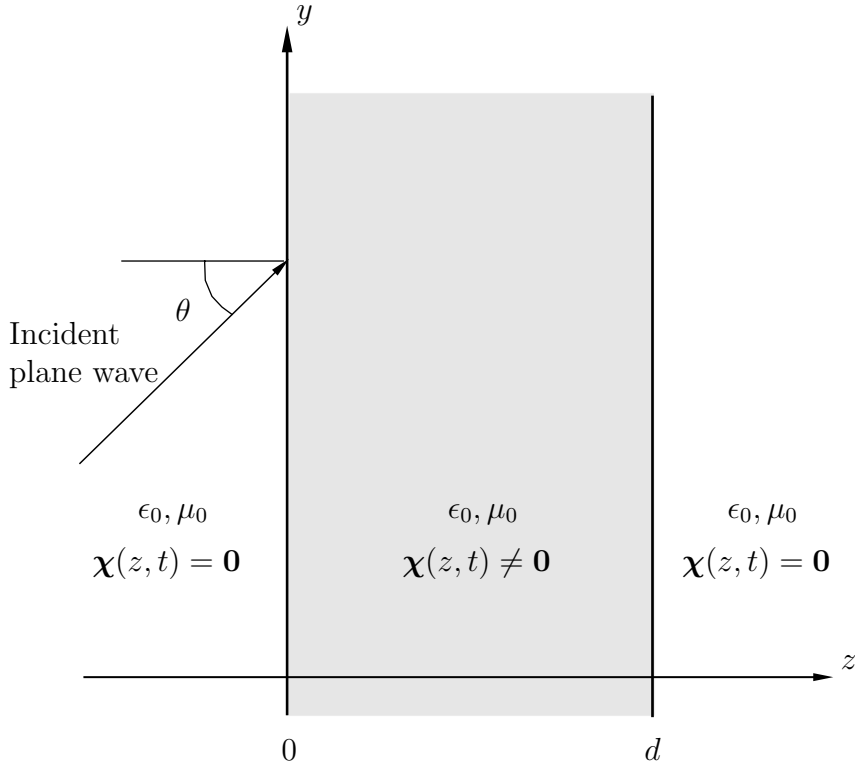


Figure 1: Geometry of the problem.

respectively. For the more general situation with a general (constant) permittivity ϵ and permeability μ inside and outside the medium, simply replace ϵ_0 by $\epsilon\epsilon_0$ and μ_0 by $\mu\mu_0$.

The medium in this paper extends from $z = 0$ to $z = d$ and is assumed to be inhomogeneous wrt depth z , (see Figure 1). The spatial variation in the susceptibility kernel χ is therefore only wrt to depth z , i.e., $\chi(\mathbf{r}, t) = \chi(z, t)$. Furthermore, there is no phase velocity mismatch at the boundaries of the slab.

An incident field impinges obliquely on the slab. The y -axis is chosen so that the plane of incidence coincides with the yz -plane and the angle of incidence is denoted θ , (see Figure 1).

All fields are assumed to vary as functions of space \mathbf{r} and time t as

$$\begin{aligned} \mathbf{E}(\mathbf{r}, t) &= \hat{x}E_x(z, s) + \hat{y}E_y(z, s) + \hat{z}E_z(z, s) \\ \mathbf{H}(\mathbf{r}, t) &= \hat{x}H_x(z, s) + \hat{y}H_y(z, s) + \hat{z}H_z(z, s) \end{aligned}$$

where θ is the angle of incidence and

$$s = t - \frac{y \sin \theta}{c_0}$$

This assumption implies that the fields at a certain point and time (\mathbf{r}, t) are identical to the fields at an earlier time $t - y \sin \theta / c_0$ at the point $y = 0$ and depth z . Therefore, at constant depth z , the history of the fields are translated in time with $y \sin \theta / c_0$.

The time convolutions in the constitutive relations, (2.2), are also changed and

$$\begin{aligned} \sum_{j=1}^3 \int_{-\infty}^t \chi_{ij}(\mathbf{r}, t - t') E_j(\mathbf{r}, t') dt' &= \sum_{j=1}^3 \int_{-\infty}^t \chi_{ij}(z, t - t') E_j(z, t' - y \sin \theta / c_0) dt' \\ &= \sum_{j=1}^3 \int_{-\infty}^s \chi_{ij}(z, s - s') E_j(z, s') ds' = (\boldsymbol{\chi}(z, \cdot) * \mathbf{E}(z, \cdot) |_i)(s) \end{aligned}$$

With this notation the x -, y - and t -differentiations transform into

$$\begin{cases} \partial_x = 0 \\ \partial_y = -\frac{\sin \theta}{c_0} \partial_s \\ \partial_t = \partial_s \end{cases}$$

In terms of the variables z and s the Maxwell equations are

$$\begin{pmatrix} 0 & -c_0 \partial_z & -\sin \theta \partial_s \\ c_0 \partial_z & 0 & 0 \\ \sin \theta \partial_s & 0 & 0 \end{pmatrix} \mathbf{E}(z, s) = -\eta_0 \partial_s \mathbf{H}(z, s) \quad (2.3)$$

$$\begin{pmatrix} 0 & -c_0 \partial_z & -\sin \theta \partial_s \\ c_0 \partial_z & 0 & 0 \\ \sin \theta \partial_s & 0 & 0 \end{pmatrix} \eta_0 \mathbf{H}(z, s) = \partial_s (\mathbf{E}(z, s) + (\boldsymbol{\chi}(z, \cdot) * \mathbf{E}(z, \cdot))(s)) \quad (2.4)$$

The objective is now to eliminate the third components of the fields \mathbf{E} and \mathbf{H} . To accomplish this, it is convenient to adopt a 2×2 matrix notation. The first and second components of (2.3) and (2.4) are

$$\begin{cases} c_0 \partial_z \mathbf{J} \mathbf{E}_{\parallel} - \sin \theta \partial_s \begin{pmatrix} E_3 \\ 0 \end{pmatrix} = -\eta_0 \partial_s \mathbf{H}_{\parallel} \\ c_0 \eta_0 \partial_z \mathbf{J} \mathbf{H}_{\parallel} - \sin \theta \eta_0 \partial_s \begin{pmatrix} H_3 \\ 0 \end{pmatrix} = \partial_s (\mathbf{E}_{\parallel} + \boldsymbol{\chi}_{\parallel} * \mathbf{E}_{\parallel}) + \partial_s \begin{pmatrix} \chi_{13} * E_3 \\ \chi_{23} * E_3 \end{pmatrix} \end{cases} \quad (2.5)$$

where \mathbf{J} is defined as

$$\mathbf{J} = \begin{pmatrix} 0 & -1 \\ 1 & 0 \end{pmatrix}$$

and \mathbf{E}_{\parallel} , \mathbf{H}_{\parallel} and $\boldsymbol{\chi}_{\parallel}$ are

$$\mathbf{E}_{\parallel} = \begin{pmatrix} E_1 \\ E_2 \end{pmatrix}, \quad \mathbf{H}_{\parallel} = \begin{pmatrix} H_1 \\ H_2 \end{pmatrix}, \quad \boldsymbol{\chi}_{\parallel} = \begin{pmatrix} \chi_{11} & \chi_{12} \\ \chi_{21} & \chi_{22} \end{pmatrix}$$

The matrix \mathbf{J} represents a right angle rotation around the z -axis. The third components of (2.3) and (2.4) are

$$\begin{cases} \eta_0 \partial_s H_3 = -\sin \theta \partial_s E_1 \\ \partial_s (E_3 + \chi_{33} * E_3) = \partial_s (\sin \theta \eta_0 H_1 - \chi_{31} * E_1 - \chi_{32} * E_2) \end{cases}$$

Integration of these equations wrt s implies

$$\begin{cases} \eta_0 H_3 = -\sin \theta E_1 \\ E_3 + \chi_{33} * E_3 = \sin \theta \eta_0 H_1 - \chi_{31} * E_1 - \chi_{32} * E_2 \end{cases}$$

since the contributions at $s \rightarrow -\infty$ all vanish. The resolvent L of the kernel χ_{33} is defined by the Volterra equation of the second kind

$$L(z, s) + \chi_{33}(z, s) + (L(z, \cdot) * \chi_{33}(z, \cdot))(s) = 0$$

This is used to express the third component of the electric and magnetic fields in terms of their first and second components.

$$\begin{cases} \eta_0 H_3 = -\sin \theta E_1 \\ E_3 = (1 + L*) (\sin \theta \eta_0 H_1 - \chi_{31} * E_1 - \chi_{32} * E_2) \end{cases} \quad (2.6)$$

The field equations in (2.5) can therefore be expressed in just the first and second (planar) components of the electric and magnetic fields. The result is

$$c_0 \begin{pmatrix} \mathbf{J} & 0 \\ 0 & \mathbf{J} \end{pmatrix} \partial_z \begin{pmatrix} \mathbf{E}_{\parallel} \\ \eta_0 \mathbf{H}_{\parallel} \end{pmatrix} = \begin{pmatrix} \mathbf{D}_{11} & \mathbf{D}_{12} \\ \mathbf{D}_{21} & \mathbf{D}_{22} \end{pmatrix} \partial_s \begin{pmatrix} \mathbf{E}_{\parallel} \\ \eta_0 \mathbf{H}_{\parallel} \end{pmatrix} \quad (2.7)$$

where \mathbf{J} is given above and \mathbf{D}_{ij} are 2×2 matrices

$$\begin{cases} \mathbf{D}_{11} = -\sin \theta \begin{pmatrix} (1 + L*)\chi_{31}* & (1 + L*)\chi_{32}* \\ 0 & 0 \end{pmatrix} \\ \mathbf{D}_{12} = -\begin{pmatrix} \cos^2 \theta & 0 \\ 0 & 1 \end{pmatrix} + \sin^2 \theta \begin{pmatrix} L* & 0 \\ 0 & 0 \end{pmatrix} \\ \mathbf{D}_{21} = \left[\begin{pmatrix} \cos^2 \theta & 0 \\ 0 & 1 \end{pmatrix} + \boldsymbol{\chi}_{\parallel} * - \begin{pmatrix} \chi_{13} * (1 + L*)\chi_{31}* & \chi_{13} * (1 + L*)\chi_{32}* \\ \chi_{23} * (1 + L*)\chi_{31}* & \chi_{23} * (1 + L*)\chi_{32}* \end{pmatrix} \right] \\ \mathbf{D}_{22} = \sin \theta \begin{pmatrix} \chi_{13} * (1 + L*) & 0 \\ \chi_{23} * (1 + L*) & 0 \end{pmatrix} \end{cases}$$

Equation (2.7) is the basic equation for the wave propagation in the medium. The solution to this system of equations gives the x - and y -components of the electric and the magnetic fields. The z -components are then determined by (2.6).

3 Wave splitting

In this section the wave splitting concept is presented. The aim of the wave splitting is to diagonalize the vacuum terms in the Maxwell equations. Therefore, before the formal definition of the wave splitting is introduced it is relevant to study the form of the equations in free space, i.e., vacuum. The observations obtained in vacuum then motivate the formal definition of the split fields \mathbf{E}^{\pm} . This analysis is analogous to that in ref. [15].

In vacuum the Maxwell equations (2.7) simplify to

$$v\partial_z \begin{pmatrix} \mathbf{E}_{\parallel} \\ \eta_0 \mathbf{J} \mathbf{H}_{\parallel} \end{pmatrix} = \begin{pmatrix} \mathbf{0} & \mathbf{\Gamma} \\ \mathbf{\Gamma}^{-1} & \mathbf{0} \end{pmatrix} \partial_s \begin{pmatrix} \mathbf{E}_{\parallel} \\ \eta_0 \mathbf{J} \mathbf{H}_{\parallel} \end{pmatrix} \quad (3.1)$$

since $\mathbf{J}^2 = -\mathbf{I}$, where \mathbf{I} is the 2×2 identity matrix and

$$\mathbf{\Gamma} = \begin{pmatrix} \frac{1}{\cos \theta} & 0 \\ 0 & \cos \theta \end{pmatrix}, \quad v = \frac{c_0}{\cos \theta}$$

Elimination of the magnetic field implies

$$v^2 \partial_z^2 \mathbf{E}_{\parallel} = \partial_s^2 \mathbf{E}_{\parallel}$$

or

$$(v\partial_z + \partial_s)(v\partial_z - \partial_s)\mathbf{E}_{\parallel} = \mathbf{0}$$

The general solution for this system of second order equations is

$$\mathbf{E}_{\parallel} = \mathbf{E}^+(z - vs) + \mathbf{E}^-(z + vs)$$

For \mathbf{H}_{\parallel} the same result is obtained. Obviously, $v\partial_z = \mp\partial_s$ in free space. A formal integration wrt s of (3.1) then implies

$$\eta_0 \mathbf{J} \mathbf{H}^{\pm} = \mp \mathbf{\Gamma}^{-1} \mathbf{E}^{\pm}$$

The x - and y -components of the fields are then related by

$$\begin{pmatrix} \mathbf{E}_{\parallel} \\ \eta_0 \mathbf{J} \mathbf{H}_{\parallel} \end{pmatrix} = \begin{pmatrix} \mathbf{I} & \mathbf{I} \\ -\mathbf{\Gamma}^{-1} & \mathbf{\Gamma}^{-1} \end{pmatrix} \begin{pmatrix} \mathbf{E}^+ \\ \mathbf{E}^- \end{pmatrix}$$

with the inverse

$$\begin{pmatrix} \mathbf{E}^+ \\ \mathbf{E}^- \end{pmatrix} = \mathbf{P} \begin{pmatrix} \mathbf{E}_{\parallel} \\ \eta_0 \mathbf{J} \mathbf{H}_{\parallel} \end{pmatrix} \quad (3.2)$$

where the 4×4 matrix \mathbf{P} is

$$\mathbf{P} = \frac{1}{2} \begin{pmatrix} \mathbf{I} & -\mathbf{\Gamma} \\ \mathbf{I} & \mathbf{\Gamma} \end{pmatrix}$$

Equation (3.2) is the formal definition of the wave splitting. In free space, i.e., in vacuum, the transformation projects out the right and left moving parts of the solution. These parts of the field correspond to fields that have sources to the left and to the right, respectively, of the point of observation. At a point inside the dispersive slab, where $\boldsymbol{\chi} \neq \mathbf{0}$, the wave splitting, (3.2), is still well defined, but no interpretation, however, in left and right moving parts can be made. It should also be noted that the split fields \mathbf{E}^{\pm} are linear combinations of the electric and the magnetic fields \mathbf{E}_{\parallel} and \mathbf{H}_{\parallel} . It is, however, convenient to keep the notation of the electric field, even though they are not purely electric fields.

The new transformed fields \mathbf{E}^{\pm} , defined by (3.2), satisfy a system of first order hyperbolic equations, equivalent to the Maxwell equations (2.7),

$$v\partial_z \begin{pmatrix} \mathbf{E}^+ \\ \mathbf{E}^- \end{pmatrix} = \mathcal{D} \partial_s \begin{pmatrix} \mathbf{E}^+ \\ \mathbf{E}^- \end{pmatrix} \quad (3.3)$$

where the matrix-valued operator \mathcal{D} has the form

$$\mathcal{D} = \begin{pmatrix} -\mathbf{I} & 0 \\ 0 & \mathbf{I} \end{pmatrix} + \begin{pmatrix} \Delta_{11} & \Delta_{12} \\ \Delta_{21} & \Delta_{22} \end{pmatrix}^*$$

The Δ_{kl} matrices have the explicit form

$$\Delta_{kl} = (-1)^k \Delta_{\perp} + \Delta_{\parallel,kl}$$

where

$$\Delta_{\perp} = \frac{1}{2 \cos \theta} \Gamma \left[\chi_{\parallel} - \begin{pmatrix} \chi_{13} * (1 + L^*) \chi_{31} & \chi_{13} * (1 + L^*) \chi_{32} \\ \chi_{23} * (1 + L^*) \chi_{31} & \chi_{23} * (1 + L^*) \chi_{32} \end{pmatrix} \right]$$

and

$$\Delta_{\parallel,kl} = \frac{\tan \theta}{2 \cos \theta} \Gamma \left[(1 + L^*) \begin{pmatrix} 0 & (-1)^{k+l} \chi_{13} \\ \chi_{31} & \chi_{32} + (-1)^{k+l} \chi_{23} \end{pmatrix} - \tan \theta (-1)^l \begin{pmatrix} 0 & 0 \\ 0 & L \end{pmatrix} \right]$$

4 Propagation of wave front

The propagation of the wave front in a general anisotropic medium motivates special attention and treatment. Any finite jump discontinuity in the field, i.e., a wave front, attenuates and rotates as the wave propagates into the medium. This is a characteristic property of the medium and in the Appendix A the explicit expressions of these quantities are presented.

The dynamics of the plus and minus fields \mathbf{E}^{\pm} satisfy the system of equations in (3.3), which is a non-local hyperbolic PDE. Weak solutions can therefore occur along the characteristics $s \mp z/v = \xi_{\pm} = \text{constant}$. The coordinates ξ_{\pm} are the characteristic coordinates of the system (3.3). Any finite jump discontinuity in a field is denoted by a square bracket, i.e.,

$$[\mathbf{E}^+(z, s)] = \mathbf{E}^+(z, s^+) - \mathbf{E}^+(z, s^-) \quad (4.1)$$

Propagation of singularity arguments show that the finite jump discontinuities satisfy the following system of first order equations

$$\frac{d}{dz} [\mathbf{E}^{\pm}(z, \xi_{\pm} \pm z/v)] + \mathbf{a}^{\pm}(z) [\mathbf{E}^{\pm}(z, \xi_{\pm} \pm z/v)] = \mathbf{0} \quad (4.2)$$

where

$$\begin{cases} \mathbf{a}^+(z) = -\frac{1}{v} \Delta_{11}(z, 0^+) \\ \mathbf{a}^-(z) = -\frac{1}{v} \Delta_{22}(z, 0^+) \end{cases}$$

The other components of the matrix-valued operator, Δ_{12} and Δ_{21} , do not affect the propagation of the finite jump discontinuity.

The physical interpretation of this result becomes simpler if the following equivalent representation of the solution is used.

$$[\mathbf{E}^\pm(z_2, \xi_\pm \pm z_2/v)] = \mathbf{Q}^\pm(z_1, z_2) [\mathbf{E}^\pm(z_1, \xi_\pm \pm z_1/v)]$$

where the matrices $\mathbf{Q}^\pm(z_1, z_2)$ satisfy

$$\begin{cases} \frac{d}{dz_2} \mathbf{Q}^\pm(z_1, z_2) + \mathbf{a}^\pm(z_2) \mathbf{Q}^\pm(z_1, z_2) = \mathbf{0} \\ \mathbf{Q}^\pm(z_1, z_1) = \mathbf{I} \end{cases} \quad (4.3)$$

The unique solubility and equivalence of these equations are examined in, e.g., [3, 8]. The main results for general χ are found in Appendix A. Note the structure of the differentiation rules (A.2) of the \mathbf{Q} matrices. This is exactly what is needed to construct the imbedding and Green functions equations. For some media there is an exact solution of \mathbf{Q}^\pm in terms of the exponential function of a 2×2 matrix. This solution is further developed in Appendix B. It is pointed out in Appendix B that the wave front may be decomposed (for some media) as an attenuation factor times an element in $SL(2, \mathbb{R})$ (the two-dimensional Lorentz group), which may be viewed as 2 rotations and between them a contraction/dilation term. With the notation

$$-\int_{z_1}^{z_2} \mathbf{a}^+(z) dz = \begin{pmatrix} \alpha + \beta & \gamma + \delta \\ \gamma - \delta & \alpha - \beta \end{pmatrix}$$

the result is

$$\mathbf{Q}^+(z_1, z_2) = e^\alpha \begin{pmatrix} \cos \varphi_2 & \sin \varphi_2 \\ -\sin \varphi_2 & \cos \varphi_2 \end{pmatrix} \begin{pmatrix} e^\eta & 0 \\ 0 & e^{-\eta} \end{pmatrix} \begin{pmatrix} \cos \varphi_1 & \sin \varphi_1 \\ -\sin \varphi_1 & \cos \varphi_1 \end{pmatrix}$$

with

$$\begin{cases} \sinh \eta \cos(\varphi_1 - \varphi_2) = \beta \frac{\sinh \xi}{\xi} \\ \sinh \eta \sin(\varphi_1 - \varphi_2) = \gamma \frac{\sinh \xi}{\xi} \\ \cosh \eta \sin(\varphi_1 + \varphi_2) = \delta \frac{\sinh \xi}{\xi} \end{cases}$$

where

$$\xi = \sqrt{\beta^2 + \gamma^2 - \delta^2}$$

A similar result holds for the \mathbf{Q}^- matrix.

5 Imbedding equations

The imbedding approach uses the idea of studying a one-parameter family of scattering problems. Specifically a subsection $[z, d]$ of the physical slab $[0, d]$ is considered (see Figure 2). As the parameter z varies from 0 to d , the subsection varies from the

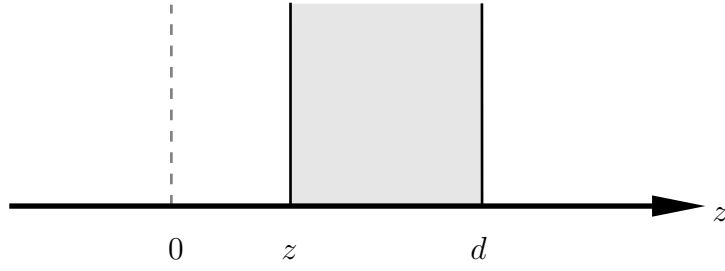


Figure 2: The imbedding geometry.

full physical slab to the case where no slab is present. At one endpoint of the parameter ($z = d$), the scattering problem is trivial, while at the other endpoint ($z = 0$), the full scattering problem is solved. This approach has been used extensively during the last decade, see [1, 4, 20].

For a subsection $[z, d]$ the 2×2 matrix-valued reflection and transmission kernels $\mathbf{R}(z, s)$ and $\mathbf{T}(z, s)$, respectively, are defined as ($z \in (0, d), s > 0$)

$$\begin{aligned} \mathbf{E}^-(z, s) &= \mathbf{R}(z, \cdot) * \mathbf{E}^+(z, \cdot)(s) \\ \mathbf{E}^+(d, s + (d - z)/v) &= \mathbf{Q}^+(z, d) \{ \mathbf{E}^+(z, s) + \mathbf{T}(z, \cdot) * \mathbf{E}^+(z, \cdot)(s) \} \end{aligned}$$

The physical reflection and transmission kernels are $\mathbf{R}(0, s)$ and $\mathbf{T}(0, s)$, respectively. Due to causality, \mathbf{R} and \mathbf{T} are identically zero for $s < 0$.

These definitions in combination with the equations (3.3) give

$$\begin{aligned} v\partial_z \mathbf{R} - 2\partial_s \mathbf{R} &= \partial_s \Delta_{21} + \partial_s \{ \Delta_{22} * \mathbf{R} - \mathbf{R} * \Delta_{11} - \mathbf{R} * \Delta_{12} * \mathbf{R} \} \\ v\partial_z \mathbf{T} &= -\partial_s \Delta_{11} - v\mathbf{a}^+ \mathbf{T} - \partial_s \{ (\mathbf{I} + \mathbf{T}^*) \Delta_{12} * \mathbf{R} + \mathbf{T} * \Delta_{11} \} \end{aligned}$$

The initial values satisfy

$$\begin{aligned} \mathbf{R}(z, 0^+) &= -\frac{1}{2} \Delta_{21}(z, 0^+) \\ \frac{d}{dz} \mathbf{T}(z, 0^+) &= \mathbf{T}(z, 0^+) \mathbf{a}^+(z) - \mathbf{a}^+(z) \mathbf{T}(z, 0^+) \\ &\quad - \frac{1}{v} \partial_s \Delta_{11}(z, 0^+) + \frac{1}{2v} \Delta_{12}(z, 0^+) \Delta_{21}(z, 0^+) \end{aligned}$$

where the second equation is obtained from the imbedding equation of the transmission kernel. At $z = d$ the boundary values are

$$\begin{aligned} \mathbf{R}(d, s) &= \mathbf{0} \\ \mathbf{T}(d, s) &= \mathbf{0} \end{aligned}$$

which corresponds to the absence of scattering. The reflection kernel has a finite jump discontinuity on the characteristic $s = 2(d - z)/v$ in the t - z -plane. Using the notation (4.1) the governing equation for the propagation of the finite jump discontinuity is

$$\frac{d}{dz} [\mathbf{R}(z, 2(d - z)/v)] = [\mathbf{R}(z, 2(d - z)/v)] \mathbf{a}^+(z) - \mathbf{a}^-(z) [\mathbf{R}(z, 2(d - z)/v)]$$

The equations for the finite jump discontinuity in \mathbf{R} and the initial value in \mathbf{T} are solved using the differentiation rules for the \mathbf{Q}^\pm matrices (see (A.2)). The results are

$$\begin{aligned} [\mathbf{R}(z, 2(d-z)/v)] &= \frac{1}{2} \mathbf{Q}^-(d, z) \mathbf{\Delta}_{21}(d, 0^+) \mathbf{Q}^+(z, d) \\ \mathbf{T}(z, 0^+) &= \frac{1}{v} \int_z^d \mathbf{Q}^+(z', z) \left\{ \partial_s \mathbf{\Delta}_{11}(z', 0^+) - \frac{1}{2} \mathbf{\Delta}_{12}(z', 0^+) \mathbf{\Delta}_{21}(z', 0^+) \right\} \mathbf{Q}^+(z, z') dz' \end{aligned}$$

It must be stressed that $\mathbf{R}(0, t)$ and $\mathbf{T}(0, t)$ of the above equations are the reflection and the transmission kernels for the components of the electromagnetic field along the plane of stratification. The total scattered fields may be constructed by noting that the reflected electric field at the left edge of the slab is

$$\mathbf{E}^r(0^-, t) = \hat{x} E_x^-(0, t) + \hat{y} E_y^-(0, t) + \hat{z} \tan \theta E_y^-(0, t)$$

and that the transmitted electric field at the right edge of the slab is

$$\mathbf{E}^t(d^+, t) = \hat{x} E_x^+(d, t) + \hat{y} E_y^+(d, t) - \hat{z} \tan \theta E_y^+(d, t)$$

5.1 Homogeneous semi-infinite slab, normal incidence

In the case of a homogeneous, $\chi(z, t) = \chi(t)$, semi-infinite slab ($d \rightarrow \infty$) the reflection kernel is independent of z and the imbedding equation simplifies. Only total time derivatives remain. Integrating wrt time the \mathbf{R} -equation for normal incidence becomes

$$2\mathbf{R} + \mathbf{\Delta}_\perp + \mathbf{\Delta}_\perp * \mathbf{R} + \mathbf{R} * \mathbf{\Delta}_\perp + \mathbf{R} * \mathbf{\Delta}_\perp * \mathbf{R} = \mathbf{0}$$

This equation, which is similar to the Riccati equation, has some interesting symmetries. The transpose of \mathbf{R} satisfies the same equation with $\mathbf{\Delta}_\perp$ replaced by its transpose $\mathbf{\Delta}_\perp^T$. For a reciprocal medium and normal incidence $\mathbf{\Delta}_\perp = \mathbf{\Delta}_\perp^T$. Hence, in this special case, \mathbf{R} is a symmetric matrix-valued function. Another symmetry is realized by taking the Laplace transform of the above equation. The matrix inverse $\{\tilde{\mathbf{R}}\}^{-1}$ satisfies the same equation as $\tilde{\mathbf{R}}$ (tilde denotes Laplace transform).

6 The Green functions

In the imbedding approach integral operators are derived that map, for a subsection, the incoming field $\mathbf{E}^+(z, s)$ to the scattered fields $\mathbf{E}^-(z, s)$ and $\mathbf{E}^+(d, s)$. The equations are obtained by varying the left endpoint of the subsection. Another approach is to introduce Green operators which map the incoming field $\mathbf{E}^+(0, s)$ to the split internal fields $\mathbf{E}^\pm(z, s)$ at an arbitrary depth z , see Refs [13, 16]. The definition of the Green operators, represented in integral form with kernels $\mathbf{G}^\pm(z, s')$, respectively, are

$$\begin{aligned} \mathbf{E}^+(z, s' + z/v) &= \mathbf{Q}^+(0, z) \mathbf{E}^+(0, s') + \mathbf{G}^+(z, \cdot) * \mathbf{Q}^+(0, z) \mathbf{E}^+(0, \cdot)(s') \\ \mathbf{E}^-(z, s' + z/v) &= \mathbf{G}^-(z, \cdot) * \mathbf{Q}^+(0, z) \mathbf{E}^+(0, \cdot)(s') \end{aligned}$$

Here s' is time measured from the arrival of the wave front at z , i.e. $s' = s - z/v$, ($z \in (0, d)$, $s' > 0$). This change of time coordinate simplifies the comparison with the results of the imbedding method. The first term in the right going field is the direct response of the medium (the wave front propagating at vacuum light speed) and the other terms give the split components of the delayed response of the medium at z . For a delta function excitation, $\mathbf{G}^\pm(z, s)\mathbf{Q}^+(0, z)$ give the two split components of the delayed response.

Combined use of the definitions above and (3.3) give

$$\begin{aligned} v\partial_z \mathbf{G}^+ &= \mathbf{G}^+ v\mathbf{a}^+ + \partial_{s'} \{ \Delta_{11} + \Delta_{11} * \mathbf{G}^+ + \Delta_{12} * \mathbf{G}^- \} \\ v\partial_z \mathbf{G}^- - 2\partial_{s'} \mathbf{G}^- &= \mathbf{G}^- v\mathbf{a}^+ + \partial_{s'} \{ \Delta_{21} + \Delta_{21} * \mathbf{G}^+ + \Delta_{22} * \mathbf{G}^- \} \end{aligned}$$

Due to causality, \mathbf{G}^\pm are identically zero for $s' < 0$. The initial values satisfy

$$\begin{aligned} \mathbf{G}^-(z, 0^+) &= -\frac{1}{2}\Delta_{21}(z, 0^+) \\ \frac{d}{dz} \mathbf{G}^+(z, 0^+) &= \mathbf{G}^+(z, 0^+)\mathbf{a}^+(z) - \mathbf{a}^+(z)\mathbf{G}^+(z, 0^+) \\ &\quad + \frac{1}{v}\partial_{s'} \Delta_{11}(z, 0^+) - \frac{1}{2v}\Delta_{12}(z, 0^+)\Delta_{21}(z, 0^+) \end{aligned}$$

and the boundary values are

$$\begin{aligned} \mathbf{G}^+(0, s') &= \mathbf{0} \\ \mathbf{G}^-(d, s') &= \mathbf{0} \end{aligned}$$

The first boundary value is due to the definition of the Green operators and the second one corresponds to the absence of sources for $z \in (d, \infty)$. \mathbf{G}^- has a finite jump discontinuity, propagating along the characteristic $s' = 2(d - z)/v$, which satisfies the equation

$$\frac{d}{dz} [\mathbf{G}^-(z, 2(d - z)/v)] = [\mathbf{G}^-(z, 2(d - z)/v)] \mathbf{a}^+(z) - \mathbf{a}^-(z) [\mathbf{G}^-(z, 2(d - z)/v)]$$

The equations for $\mathbf{G}^+(z, 0^+)$ and $[\mathbf{G}^-]$ are similar to those for $\mathbf{T}(z, 0^+)$ and $[\mathbf{R}]$. Thus, the differentiation rules (A.2) are used again to get

$$\begin{aligned} [\mathbf{G}^-(z, 2(d - z)/v)] &= \frac{1}{2}\mathbf{Q}^-(d, z)\Delta_{21}(d, 0^+)\mathbf{Q}^+(z, d) \\ \mathbf{G}^+(z, 0^+) &= \frac{1}{v} \int_0^z \mathbf{Q}^+(z', z) \left\{ \partial_{s'} \Delta_{11}(z', 0^+) - \frac{1}{2}\Delta_{12}(z', 0^+)\Delta_{21}(z', 0^+) \right\} \mathbf{Q}^+(z, z') dz' \end{aligned}$$

6.1 Relations between scattering operators

The imbedding operators and the Green operators are related to each other. This is realized by dividing the slab in two regions $[0, z]$ and $[z, d]$. Using Green operators

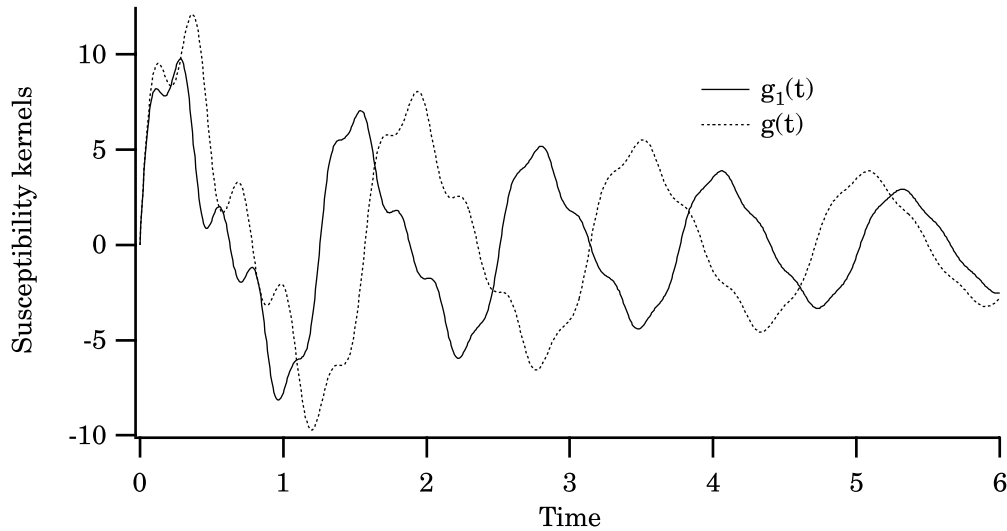


Figure 3: The kernels $g_1(t)$ and $g(t)$ for the Lorentz medium in Example 1. The time scale is given in units of d/c_0 , and the vertical axis in units of c_0/d .

in the left and imbedding operators in the right region the following equations are obtained

$$\begin{aligned}\mathbf{G}^-(z, s) &= \mathbf{R}(z, s) + \mathbf{R}(z, \cdot) * \mathbf{G}^+(z, \cdot)(s) \\ \mathbf{Q}^+(d, z)\mathbf{G}^+(d, s)\mathbf{Q}^+(z, d) &= \mathbf{G}^+(z, s) + \mathbf{T}(z, s) + \mathbf{T}(z, \cdot) * \mathbf{G}^+(z, \cdot)(s)\end{aligned}$$

The boundary values at $z = 0$ are

$$\begin{aligned}\mathbf{G}^-(0, s) &= \mathbf{R}(0, s) \\ \mathbf{G}^+(d, s) &= \mathbf{Q}^+(0, d)\mathbf{T}(0, s)\mathbf{Q}^+(d, 0)\end{aligned}$$

These equations can be used to obtain efficient numerical algorithms (see Ref. [11]).

7 Numerical experiment

In this section some numerical examples of the direct scattering problem are presented. Given a specific dispersive medium, $\chi(z, s)$, the reflection and transmission kernels are calculated. The first examples, 1-3, are all uniaxial, homogeneous media which correspond to trigonal, tetragonal and hexagonal crystal structure respectively (see Ref. [2]). These media are all reciprocal. In Example 4 scattering by a non-reciprocal, homogeneous medium is presented, see also Ref. [10].

Example 1

The first example illustrates scattering by a uniaxial medium at normal incidence, $\theta = 0$. The susceptibility kernel along the optical axis is denoted $g_1(t)$, and along the

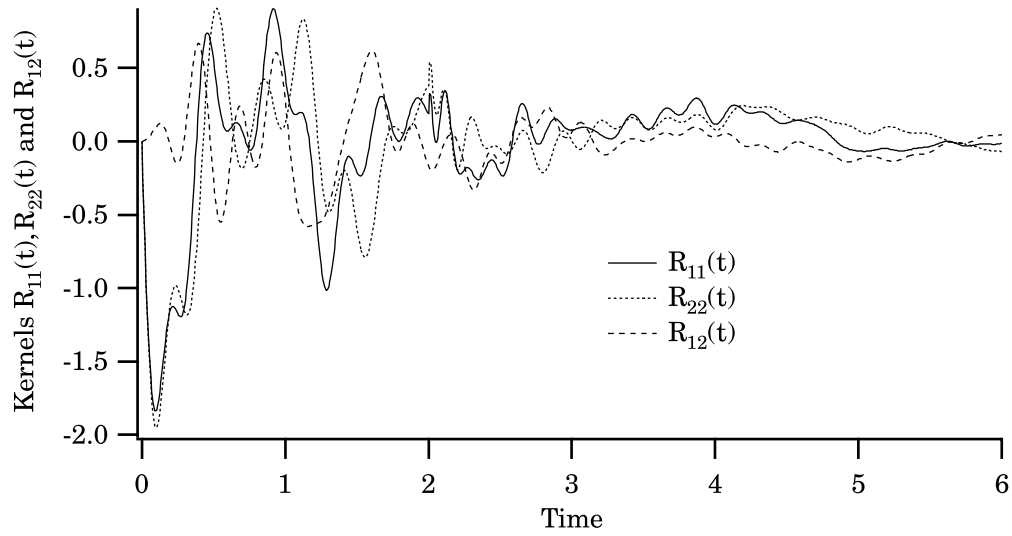


Figure 4: The reflection kernels $R_{11}(t)$, $R_{22}(t)$ and $R_{12}(t)$ for a reciprocal Lorentz medium in Example 1. The time scale is given in units of d/c_0 , and the vertical axis in units of c_0/d .

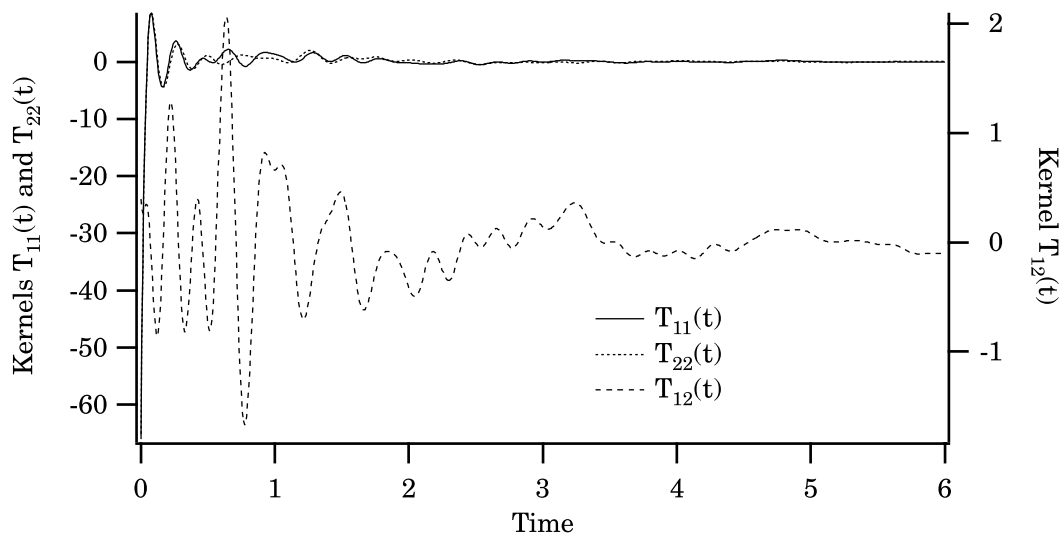


Figure 5: The transmission kernels $T_{11}(t)$, $T_{22}(t)$ and $T_{12}(t)$ for a reciprocal Lorentz medium in Example 1. The time scale is given in units of d/c_0 , and the vertical axis in units of c_0/d .

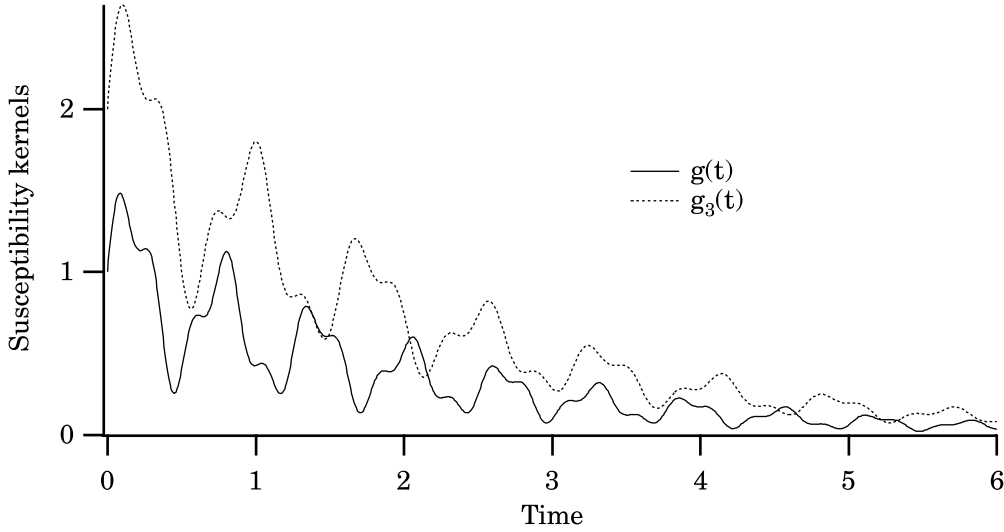


Figure 6: The kernels $g(t)$ and $g_3(t)$ for the Debye-Lorentz medium in Example 2. The time scale is given in units of d/c_0 , and the vertical axis in units of c_0/d .

other two axis the kernels are denoted $g(t)$. The optical axis of the uniaxial medium lies in the x - y -plane and the angle between the optical axis and the x -direction is ϕ , i.e., the susceptibility matrix in the rectangular coordinate system is

$$\chi(t) = \begin{pmatrix} g_1(t) \cos^2 \phi + g(t) \sin^2 \phi & (g_1(t) - g(t)) \cos \phi \sin \phi & 0 \\ (g_1(t) - g(t)) \cos \phi \sin \phi & g_1(t) \sin^2 \phi + g(t) \cos^2 \phi & 0 \\ 0 & 0 & g(t) \end{pmatrix}$$

The functions $g_1(t)$ and $g(t)$, which model a Lorentz medium, are (see also Figure 3)

$$\begin{cases} g_1(t) = 8e^{-.2t} \sin 5t + 4e^{-.5t} \sin 10t + 2e^{-.5t} \sin 25t \\ g(t) = 10e^{-.2t} \sin 4t + 4e^{-.5t} \sin 8t + 3e^{-.5t} \sin 20t \end{cases}$$

In Figure 4 the reflection kernels $R_{11}(t)$, $R_{22}(t)$ and $R_{12}(t)$ are depicted and in Figure 5 the corresponding transmission kernels when the angle $\phi = \pi/6$. Since the uniaxial medium is reciprocal and normal incidence case is considered, both kernels are symmetric, i.e., $R_{12}(t) = R_{21}(t)$ and $T_{12}(t) = T_{21}(t)$.

Example 2

This example illustrates scattering by a uniaxial medium at normal incidence, $\theta = 0$. The susceptibility kernel along the optical axis is denoted $g_3(t)$, and along the other two axis they are denoted $g(t)$. The optical axis of the uniaxial medium lies in the y - z -plane and the angle between the optical axis and the z -direction is ϕ , i.e., the susceptibility matrix in the rectangular coordinate system is

$$\chi(t) = \begin{pmatrix} g(t) & 0 & 0 \\ 0 & g(t) \cos^2 \phi + g_3(t) \sin^2 \phi & (g_3(t) - g(t)) \cos \phi \sin \phi \\ 0 & (g_3(t) - g(t)) \cos \phi \sin \phi & g(t) \sin^2 \phi + g_3(t) \cos^2 \phi \end{pmatrix}$$

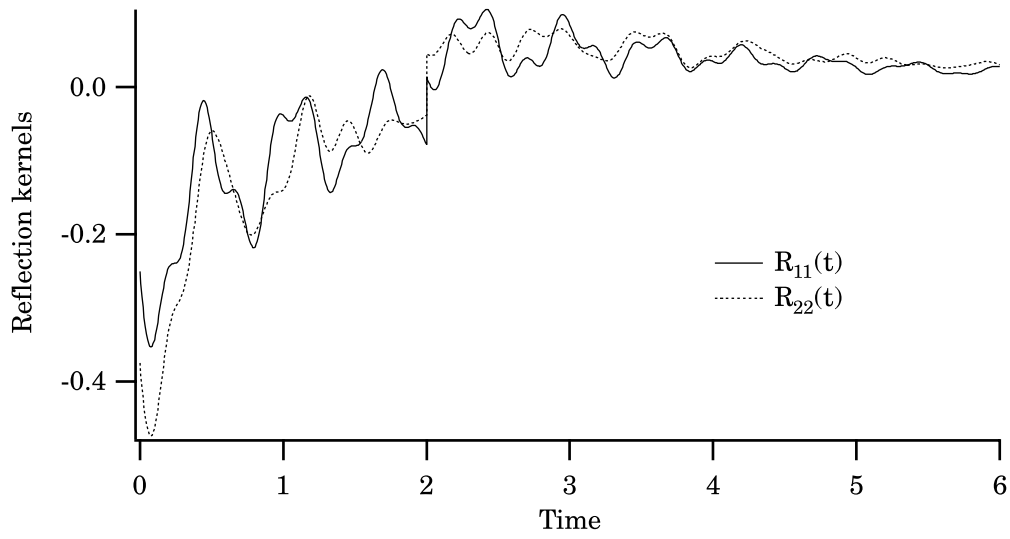


Figure 7: The reflection kernels $R_{11}(t)$ and $R_{22}(t)$ for a reciprocal Debye-Lorentz medium in Example 2. The time scale is given in units of d/c_0 , and the vertical axis in units of c_0/d .

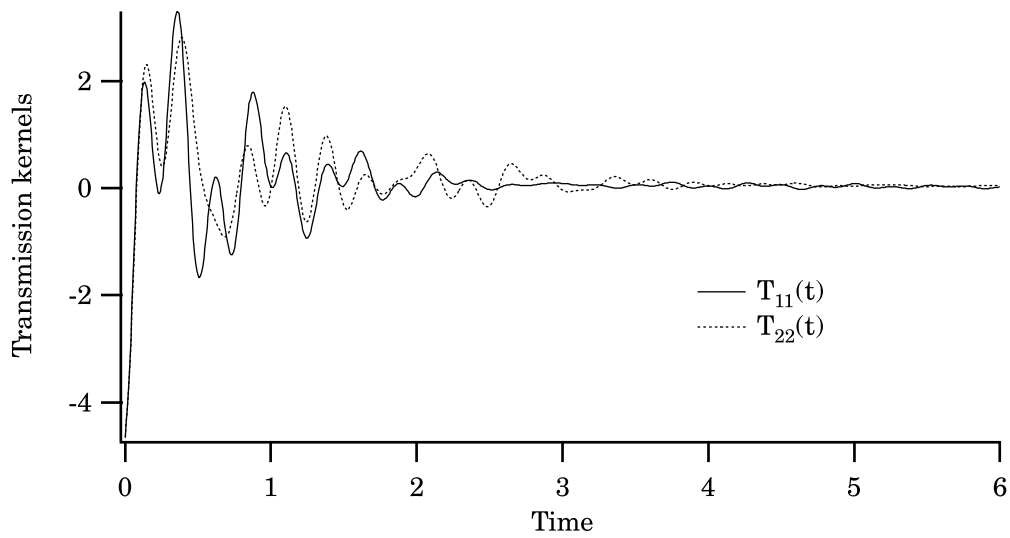


Figure 8: The transmission kernels $T_{11}(t)$ and $T_{22}(t)$ for a reciprocal Debye-Lorentz medium in Example 2. The time scale is given in units of d/c_0 , and the vertical axis in units of c_0/d .

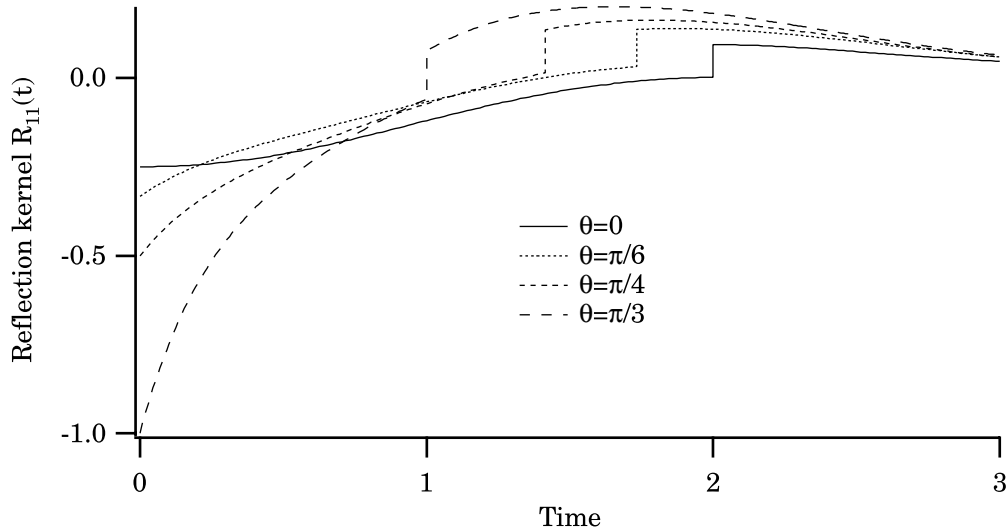


Figure 9: The reflection kernel $R_{11}(t)$ for the reciprocal Debye-Lorentz medium in Example 3. The time scale is given in units of d/c_0 , and the vertical axis in units of c_0/d .

In this example the g and g_3 functions model a Debye-Lorentz medium. They are (see also Figure 6)

$$\begin{cases} g(t) = e^{-.5t} + .5e^{-.5t} \sin 10t + .2e^{-.5t} \sin 25t \\ g_3(t) = 2e^{-.5t} + .7e^{-.5t} \sin 8t + .3e^{-.5t} \sin 20t \end{cases}$$

The scattering kernels are depicted in Figures 7 and 8, respectively, for an angle $\phi = \pi/4$. The finite jump discontinuities at $t = 2$ are due to scattering from the back wall and to the fact that $\chi_{\parallel}(t = 0^+) \neq \mathbf{0}$. Due to the special form of χ_{\parallel} , no cross polarization effects appear.

Example 3

The effect of the g_3 function on the reflection kernel \mathbf{R} is illustrated in this example. The orientation of the optical axis is the same as in Example 2, but $\phi = 0$ and the angle of incidence θ varies. The functions g and g_3 are chosen as a superposition of terms with well distinguished frequencies,

$$\begin{cases} g(t) = e^{-.5t} + .5e^{-.5t} \sin 2t \\ g_3(t) = 2e^{-.5t} + .2e^{-.5t} \sin 10t \end{cases}$$

For normal incidence, the response is that of an isotropic medium with kernel $g(t)$. As the angle θ increases, the anisotropic properties ($g \neq g_3$) enter. The reflection kernels R_{11} and R_{22} are depicted in Figures 9 and 10, respectively, for four different angles of incidence, $\theta = 0, \pi/6, \pi/4, \pi/3$. Finite jump discontinuities appear at different times corresponding to varying travel time through the slab.

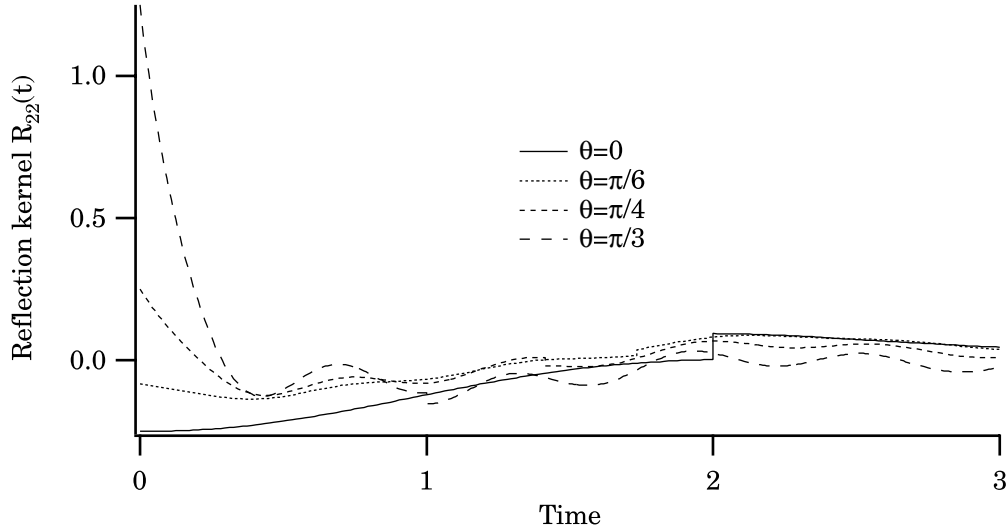


Figure 10: The reflection kernel $R_{22}(t)$ for the reciprocal Debye-Lorentz medium in Example 3. The time scale is given in units of d/c_0 , and the vertical axis in units of c_0/d .

Example 4

Scattering by a plasma with a constant magnetic induction B_0 along the z -axis, i.e., a non-reciprocal medium (gyrotropic medium), is illustrated in this last example (see Ref. [10]). Conversion of the analysis presented in Ref. [10] gives the non-zero components of χ .

$$\begin{cases} \chi_{11}(t) = \chi_{22}(t) = \omega_p^2 \frac{\nu}{\nu^2 + \omega_g^2} \left(1 - e^{-\nu t} \left(\cos \omega_g t - \frac{\omega_g}{\nu} \sin \omega_g t \right) \right) \\ \chi_{12}(t) = -\chi_{21}(t) = \omega_p^2 \frac{\omega_g}{\nu^2 + \omega_g^2} \left(1 - e^{-\nu t} \left(\cos \omega_g t + \frac{\nu}{\omega_g} \sin \omega_g t \right) \right) \\ \chi_{33}(t) = \frac{\omega_p^2}{\nu} (1 - e^{-\nu t}) \end{cases}$$

The plasma frequency ω_p and the gyrotropic frequency ω_g are given by

$$\omega_p^2 = \frac{Nq^2}{\epsilon_0 m}, \quad \omega_g = \frac{qB_0}{m}$$

where N , q and m are the electron density of the plasma and the charge and mass of the electron, respectively. Losses in the plasma are modeled by an effective collision frequency ν . The following parameters are used

$$\omega_p = 2, \quad \omega_g = 5, \quad \nu = .5$$

In Figures 11 and 12, the scattering kernels, for normal incidence ($\theta = 0$), are depicted. Symmetries of χ and normal incidence imply that $R_{12}(t) = -R_{21}(t)$, $T_{12}(t) = -T_{21}(t)$, $R_{11}(t) = R_{22}(t)$ and $T_{11}(t) = T_{22}(t)$.

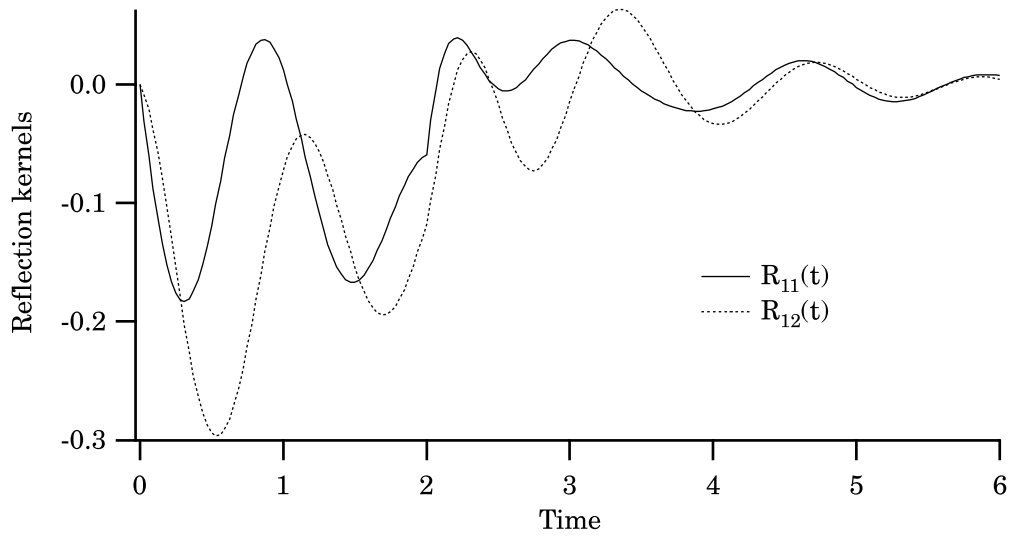


Figure 11: The reflection kernels $R_{11}(t)$ and $R_{12}(t)$ for the non-reciprocal gyrotropic medium in Example 4. The time scale is given in units of d/c_0 , and the vertical axis in units of c_0/d .

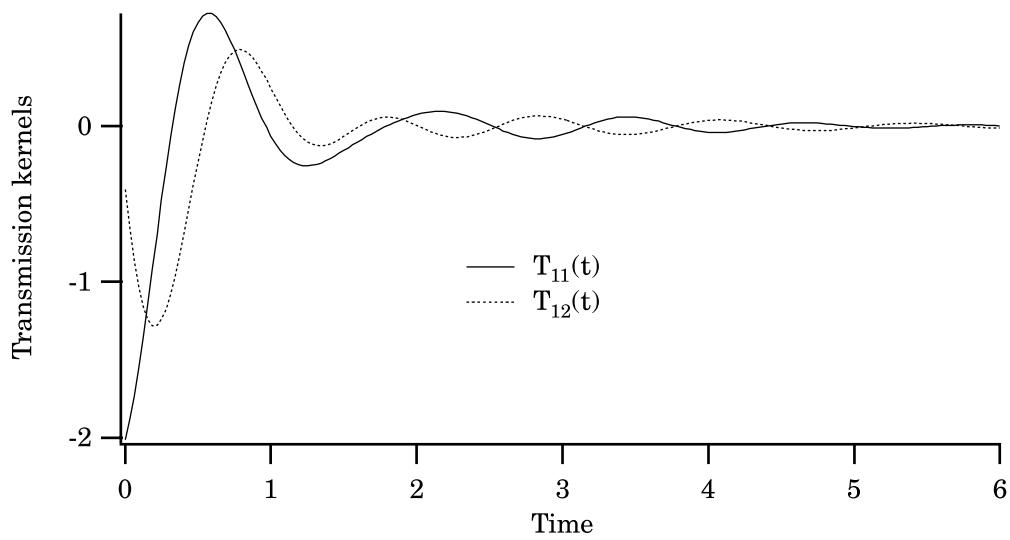


Figure 12: The transmission kernels $T_{11}(t)$ and $T_{12}(t)$ for the non-reciprocal gyrotropic medium in Example 4. The time scale is given in units of d/c_0 , and the vertical axis in units of c_0/d .

Appendix A Solution of the wave front matrix equation

It suffices to solve the equation for the matrix \mathbf{Q}^+ . The solution to the equation for \mathbf{Q}^- uses similar arguments. The \mathbf{Q}^+ -equation has the explicit form, see (4.3).

$$\begin{cases} \frac{d}{dz_2} \mathbf{Q}^+(z_1, z_2) + \mathbf{a}^+(z_2) \mathbf{Q}^+(z_1, z_2) = \mathbf{0} \\ \mathbf{Q}^+(z_1, z_1) = \mathbf{I} \end{cases} \quad (\text{A.1})$$

where

$$\mathbf{a}^+(z) = \frac{1}{2c_0} \Gamma \left[\chi_{\parallel} - \tan \theta \begin{pmatrix} 0 & \chi_{13} \\ \chi_{31} & \chi_{32} + \chi_{23} \end{pmatrix} + \tan^2 \theta \begin{pmatrix} 0 & 0 \\ 0 & \chi_{33} \end{pmatrix} \right] (z, 0^+)$$

This equation is analyzed in, e.g., [3, 8]. Transforming (A.1) into an integral equation gives

$$\mathbf{Q}^+(z_1, z_2) = \mathbf{I} - \int_{z_1}^{z_2} \mathbf{a}^+(z') \mathbf{Q}^+(z_1, z') dz'$$

Notice that the matrices $\mathbf{Q}^+(z_1, z')$ and $\mathbf{a}^+(z')$ in general do not commute. The unique solution to this integral equation exists on any compact interval I in z provided the matrix \mathbf{a}^+ is bounded, i.e.,

$$\|\mathbf{a}^+\| = \sup_{z \in I} \|a_{ij}^+(z)\| < \infty$$

where $\|a_{ij}^+(z)\|$ is any matrix norm, e.g., $\|a_{ij}\| = \max_i \sum_j |a_{ij}|$. The solution is obtained as the limit

$$\mathbf{Q}^+(z_1, z_2) = \mathbf{Q}_0^+(z_1, z_2) + \sum_{n=1}^{\infty} (\mathbf{Q}_n^+(z_1, z_2) - \mathbf{Q}_{n-1}^+(z_1, z_2)) = \lim_{n \rightarrow \infty} \mathbf{Q}_n^+(z_1, z_2)$$

where $\{\mathbf{Q}_n^+(z_1, z_2)\}_{n=0}^{\infty}$ are defined by the iteration

$$\begin{aligned} \mathbf{Q}_0^+(z_1, z_2) &= \mathbf{I} \\ \mathbf{Q}_n^+(z_1, z_2) &= \mathbf{I} - \int_{z_1}^{z_2} \mathbf{a}^+(z') \mathbf{Q}_{n-1}^+(z_1, z') dz', \quad n = 1, 2, \dots \end{aligned}$$

Cauchy's convergence test implies that the series converges, since by induction the following estimate holds

$$\|\mathbf{Q}_n^+(z_1, z_2) - \mathbf{Q}_{n-1}^+(z_1, z_2)\| \leq \frac{1}{n!} \|\mathbf{a}^+\|^n |z_2 - z_1|^n$$

This solution can also be obtained by using a spatial-ordering operator \mathcal{S} defined by

$$\mathcal{S}[\mathbf{a}^+(z') \mathbf{a}^+(z'') \dots \mathbf{a}^+(z^{(n)})] = \mathbf{a}^+(\max_i z^{(i)}) \dots \mathbf{a}^+(\min_i z^{(i)})$$

where the matrices \mathbf{a}^+ on the right hand side have been arranged in order of decreasing arguments. The solution in terms of the spatial-ordering operator then becomes

$$\mathbf{Q}^+(z_1, z_2) = \mathcal{S} \exp\left(-\int_{z_1}^{z_2} \mathbf{a}^+(z') dz'\right)$$

The unique solubility of the problem (4.2) also implies that

$$\mathbf{Q}^+(z_1, z_2) = \mathbf{Q}^+(z, z_2)\mathbf{Q}^+(z_1, z)$$

which gives the inverse

$$(\mathbf{Q}^+(z_1, z_2))^{-1} = \mathbf{Q}^+(z_2, z_1)$$

These relations can be used to obtain the expression of differentiation wrt the first argument. The rules for differentiation of the wave front matrix are then

$$\begin{cases} \frac{d}{dz_1} \mathbf{Q}^+(z_1, z_2) = \mathbf{Q}^+(z_1, z_2) \mathbf{a}^+(z_1) \\ \frac{d}{dz_2} \mathbf{Q}^+(z_1, z_2) = -\mathbf{a}^+(z_2) \mathbf{Q}^+(z_1, z_2) \end{cases} \quad (\text{A.2})$$

In some special cases one can find analytical solutions, for example if the matrix $\mathbf{a}^+(z)$ commutes in the argument, i.e.,

$$[\mathbf{a}^+(z'), \mathbf{a}^+(z'')] = \mathbf{0}, \quad z', z'' \in [z_1, z_2]$$

The solution is then

$$\mathbf{Q}^+(z_1, z_2) = \exp\left(-\int_{z_1}^{z_2} \mathbf{a}^+(z') dz'\right)$$

where the exponential function of the matrix is defined by its Taylor series. This form of the wave front matrix can then be further decomposed by means of an Iwasawa decomposition (see Appendix B).

Several special cases that satisfy this assumption are of interest. The symmetric or antisymmetric cases

$$\mathbf{a}^+(z) = \begin{pmatrix} a_{\text{co}}(z) & a_{\text{cross}}(z) \\ \pm a_{\text{cross}}(z) & a_{\text{co}}(z) \end{pmatrix}$$

are relevant models for normal incidence. The separable case

$$\mathbf{a}^+(z) = \begin{pmatrix} a_{11} & a_{12} \\ a_{21} & a_{22} \end{pmatrix} g(z)$$

is valid for any incident angle and contains the homogeneous media.

Appendix B Decomposition of the wave front matrix

In Appendix A an exact solution of the wave front matrix equation is obtained. This solution is valid in the class of media constrained by

$$[\mathbf{a}^+(z'), \mathbf{a}^+(z'')] = 0, \quad z', z'' \in [z_1, z_2]$$

The result is the exponential function of a 2×2 matrix. It is convenient to denote the matrix

$$\mathbf{A} = - \int_{z_1}^{z_2} \mathbf{a}^+(z) dz = \begin{pmatrix} \alpha + \beta & \gamma + \delta \\ \gamma - \delta & \alpha - \beta \end{pmatrix}$$

where α , β , γ and δ are real numbers.

With the notation

$$\xi = \sqrt{\beta^2 + \gamma^2 - \delta^2}$$

the exponent of the matrix \mathbf{A} can be written as

$$e^{\mathbf{A}} = e^{\alpha} \left[\sinh \xi \left(\frac{\beta}{\xi} \begin{pmatrix} 1 & 0 \\ 0 & -1 \end{pmatrix} + \frac{\gamma}{\xi} \begin{pmatrix} 0 & 1 \\ 1 & 0 \end{pmatrix} + \frac{\delta}{\xi} \begin{pmatrix} 0 & 1 \\ -1 & 0 \end{pmatrix} \right) + \cosh \xi \begin{pmatrix} 1 & 0 \\ 0 & 1 \end{pmatrix} \right]$$

This result is a decomposition of \mathbf{Q} into an attenuation factor $\exp(\alpha)$ and an element in the 2-dimensional Lorentz-group $SL(2, \mathbb{R})$. This group is an Iwasawa group and hence there are Iwasawa decompositions [17]. One possibility is

$$e^{\mathbf{A}} = e^{\alpha} \begin{pmatrix} \cos \varphi_2 & \sin \varphi_2 \\ -\sin \varphi_2 & \cos \varphi_2 \end{pmatrix} \begin{pmatrix} e^{\eta} & 0 \\ 0 & e^{-\eta} \end{pmatrix} \begin{pmatrix} \cos \varphi_1 & \sin \varphi_1 \\ -\sin \varphi_1 & \cos \varphi_1 \end{pmatrix}$$

Matrix multiplication and a comparison of the above equations give

$$\begin{cases} \sinh \eta \cos(\varphi_1 - \varphi_2) = \beta \frac{\sinh \xi}{\xi} \\ \sinh \eta \sin(\varphi_1 - \varphi_2) = \gamma \frac{\sinh \xi}{\xi} \\ \cosh \eta \sin(\varphi_1 + \varphi_2) = \delta \frac{\sinh \xi}{\xi} \end{cases}$$

For reciprocal media at normal incidence ($\theta = 0$) $\delta = 0$, since a reciprocal medium implies that \mathbf{a}^{\pm} are symmetric at normal incidence (follows from the symmetry of $\boldsymbol{\chi}$). The triple $(\varphi_2, \eta, \varphi_1)$ then degenerates to (η, φ) determined by

$$\begin{cases} \varphi_1 = -\varphi_2 = \varphi \\ \eta = \text{sign}(\beta)\xi = \text{sign}(\beta)\sqrt{\beta^2 + \gamma^2} \\ \tan(2\varphi) = \frac{\gamma}{\beta} \end{cases}$$

This defines, for each z , a coordinate system rotated an angle $\varphi(z)$ around the z -axis. In this coordinate system, the wave front is a pure contraction/dilation (the elements on the diagonal are $e^{\alpha(z) \pm \sqrt{\beta(z)^2 + \gamma(z)^2}}$) of the incoming wave front.

Appendix Acknowledgment

The work reported in this paper is supported by a grant from the Swedish Research Council for Engineering Sciences and their support is gratefully acknowledged.

References

- [1] R.S. Beezley and R.J. Krueger. An electromagnetic inverse problem for dispersive media. *J. Math. Phys.*, **26**(2), 317–325, 1985.
- [2] C.F. Bohren and D.R. Huffman. *Absorption and Scattering of Light by Small Particles*. John Wiley & Sons, New York, 1983.
- [3] E.A. Coddington and N. Levinson. *Theory of Ordinary Differential Equations*. McGraw-Hill Book Company, New York, 1955.
- [4] J.P. Coronas, M.E. Davison, and R.J. Krueger. Wave splittings, invariant imbedding and inverse scattering. In A.J. Devaney, editor, *Inverse Optics*, pages 102–106, SPIE Bellingham, WA, 1983. Proc. SPIE 413.
- [5] J.P. Coronas, G. Kristensson, P. Nelson, and D.L. Seth, editors. *Invariant Imbedding and Inverse Problems*. SIAM, 1992.
- [6] R.D. Graglia and P.L.E. Uslenghi. Electromagnetic scattering from anisotropic materials, part I: General theory. *IEEE Trans. Antennas Propagat.*, **62**, 867–869, 1984.
- [7] R.D. Graglia and P.L.E. Uslenghi. Electromagnetic scattering from anisotropic materials, part II: Computer code and numerical results in two dimensions. *IEEE Trans. Antennas Propagat.*, **AP-35**(2), 225–232, 1987.
- [8] E. Hille. *Lectures on Ordinary Differential Equations*. Addison-Wesley, Reading, 1969.
- [9] A. Karlsson and G. Kristensson. Constitutive relations, dissipation and reciprocity for the Maxwell equations in the time domain. *J. Electro. Waves Applic.*, **6**(5/6), 537–551, 1992.
- [10] A. Karlsson, H. Otterheim, and R. Stewart. Electromagnetic fields in an inhomogeneous plasma from obliquely incident transient plane waves. Technical Report TRITA-TET 91-2, Department of Electromagnetic Theory, S-100 44 Stockholm, Sweden, 1991.

- [11] A. Karlsson, H. Otterheim, and R. Stewart. Transient wave propagation in composite media: A green functions approach. Technical Report LUTEDX/(TEAT-7021)/1-27/(1992), Lund Institute of Technology, Department of Electromagnetic Theory, P.O. Box 118, S-211 00 Lund, Sweden, 1992.
- [12] J.A. Kong. Electromagnetic fields due to dipole antennas over stratified anisotropic media. *Geophysics*, **37**(6), 985–996, 1972.
- [13] G. Kristensson. Direct and inverse scattering problems in dispersive media—Green’s functions and invariant imbedding techniques. In Kleinman R., Kress R., and Martensen E., editors, *Direct and Inverse Boundary Value Problems*, Methoden und Verfahren der Mathematischen Physik, Band 37, pages 105–119, Mathematisches Forschungsinstitut Oberwolfach, FRG, 1991.
- [14] G. Kristensson and S. Rikte. Scattering of transient electromagnetic waves in reciprocal bi-isotropic media. *J. Electro. Waves Applic.*, **6**(11), 1517–1535, 1992.
- [15] G. Kristensson and S. Rikte. Transient wave propagation in reciprocal bi-isotropic media at oblique incidence. *J. Math. Phys.*, **34**(4), 1339–1359, 1993.
- [16] R.J. Krueger and R.L. Ochs, Jr. A Green’s function approach to the determination of internal fields. *Wave Motion*, **11**, 525–543, 1989.
- [17] S. Lang. *$SL_2(\mathbf{R})$* . Addison-Wesley, Reading, 1975.
- [18] J.C. Monzon. On a surface integral representation for homogeneous anisotropic regions: Two-dimensional case. *IEEE Trans. Antennas Propagat.*, **AP-36**(10), 1401–1406, 1988.
- [19] A.M. Morgan, D.L. Fischer, and E.A. Milne. Electromagnetic scattering by stratified inhomogeneous anisotropic media. *IEEE Trans. Antennas Propagat.*, **AP-35**(2), 191–197, 1987.
- [20] R.D. Stewart. *Transient electromagnetic scattering on anisotropic media*. PhD thesis, Iowa State University, Ames, Iowa, 1989.
- [21] C.-C. Su. Electromagnetic scattering by a dielectric body with arbitrary inhomogeneity and anisotropy. *IEEE Trans. Antennas Propagat.*, **AP-37**(3), 384–389, 1989.
- [22] V.H. Weston. Invariant imbedding for the wave equation in three dimensions and the applications to the direct and inverse problems. *Inverse Problems*, **6**, 1075–1105, 1990.
- [23] V.H. Weston. Invariant imbedding and wave splitting in \mathbf{R}^3 : II. the Green function approach to inverse scattering. *Inverse Problems*, **8**, 919–947, 1992.
- [24] V.H. Weston. Time-domain wave-splitting of Maxwell’s equations. *J. Math. Phys.*, **34**(4), 1370–1392, 1993.